Equilibrium Conditions in High-density Helicon Discharges

F.F. Chen, I.D. Sudit, M. Light, D.D. Blackwell, and D. Arnush

Electrical Engineering Department
University of California, Los Angeles 90024-1594

ABSTRACT

In the last two years, we have made great progress in understanding how helicon discharges work. Major results are:

1. We have solved the dispersion relation for nonuniform plasma densities. The measured density profiles are used henceforth.

2. The wave magnetic field has been measured radially for various antennas. The m = +1 azimuthal mode is preferentially excited and agrees well with theory.

3. The density, temperature, potential, and Ar II light have been measured axially for helical and straight antennas. The density peaks downstream. These data have been explained by a diffusion model of the discharge.

4. The wave magnetic field has been measured axially. The wavelength varies as expected with density. A standing wave pattern is seen which is explained by the beating of two radial modes. Antenna calculations support these observations.

5. The ANTENA code has been understood and simplified so that antenna coupling calculations can be made on a PC.

6. No Landau-accelerated fast electrons have been observed; our ionization can be explained by collisional damping alone.

7. Diagnostics have been developed and theoretically analyzed for the above measurements. A new theory shows that fast electrons which occur in pulses in phase with the RF cannot be seen with our RF-compensated Langmuir probes.

8. The helicon discharge appears to be an ideal remote source, with high density and low T_e downstream from the antenna.

Equilibrium Conditions in High-density Helicon Discharges

F.F. Chen, I.D. Sudit, M. Light, D.D. Blackwell, and D. Arnush

Electrical Engineering Department
University of California, Los Angeles 90024-1594

PAPERS IN WHICH THESE RESULTS WILL APPEAR

F.F. Chen, M.J. Hsieh, and M. Light, "Helicon waves in a nonuniform plasma," Plasma Sources Sci. Technol. **3**, 49 (1994).

I.D. Sudit and F.F. Chen, "RF compensated probes for high-density discharges," Plasma Sources Sci. Technol. **3**, 162 (1994).

I.D. Sudit and F.F. Chen, "A nonsingular helicon wave equation for a nonuniform plasma," Plasma Sources Sci. Technol. **3**, 602 (1994).

M. Light and F.F. Chen, "Helicon Wave Excitation with Helical Antennas," Phys. Plasmas **2**, 1084 (1995).

M. Light and F.F. Chen, "Axial Variation of Helicon Wave Amplitudes," Phys. Plasmas (in preparation).

I.D. Sudit and F.F. Chen, "Remote Source Characteristics of Helicon Discharges," Plasma Sources Sci. Technol. (submitted, 1995).

F.F. Chen and D.D. Blackwell, "Probe Detection of Phased EEDFs in RF Discharges," Plasma Sources Sci. Technol. (in preparation).

D. Arnush and F.F. Chen, "Antenna Coupling to Helicon Waves," (in planning stage).

The traveling wavelength of the helicon wave was measured with magnetic probe interferometry. The wavelengths measured vary inversely with the plasma density as predicted by the dispersion relation of helicon waves in uniform plasmas.

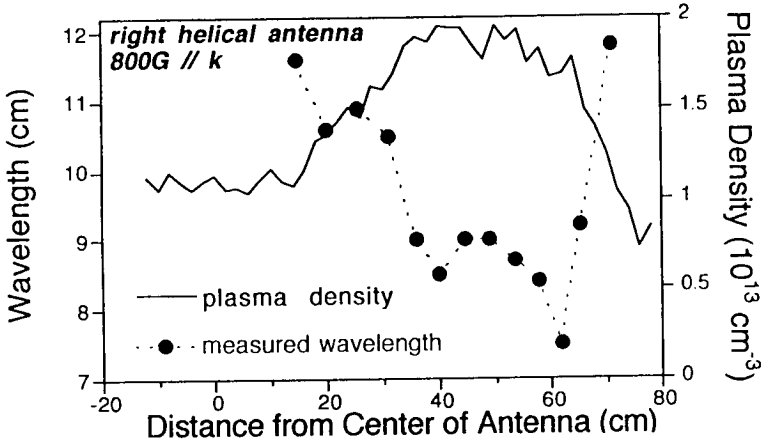

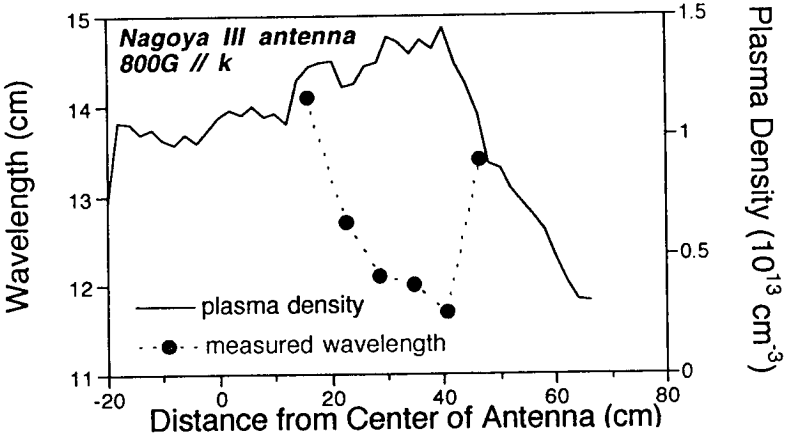

SUMMARY

1. The data clearly show the onset of the helicon (H) mode as B is increased. The B = 0 (ICP) mode is confined to the antenna region, whereas the helicon mode develops downstream.

2. The previously reported dominance of the m = +1, right-hand polarized mode is confirmed. The RH helical antenna generates a dense plasma downstream only when B is in the right direction. The Nagoya III antenna generates the m = +1 mode symmetrically in both directions.

3. Once the T_e variation is taken as given, all else makes sense. The density peaks downstream as required by pressure balance as the temperature decays. The measured n and V_s profiles give *quantitative* agreement on pressure balance, especially for the ICP mode; the H mode agrees not as well, because of the difficulty in measuring V_s in a strong B.

4. The Ar^+ light profile agrees well with that computed from the measured n and T_e profiles.

5. With measured n, T_e, and V_s, the computed diffusion loss rate agrees with the computed ionization rate, assuming no Landau damping effects. For the H mode, neutral depletion must occur.

6. The helicon wave field shows beats whose spacing agrees with the simultaneous launching of two radial m = +1 modes, each satisfying the nonuniform-plasma dispersion relation. The local wavelength of the main mode varies with *n* as expected.

The remaining problems are:

1. Can we explain the T_e falloff rate?
2. Can we explain the wave damping length?
3. Can we design a probe that can detect *phased* fast electrons?

The magnetic probe measurements of the helicon wave reveal a standing wave pattern that develops as the axial dc magnetic field increases. The decreasing wave amplitude suggests that the pattern is not due to reflections at the end of the discharge.

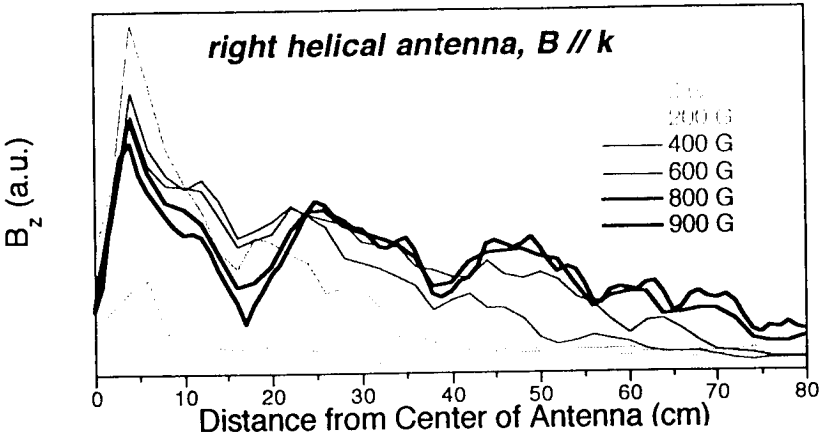

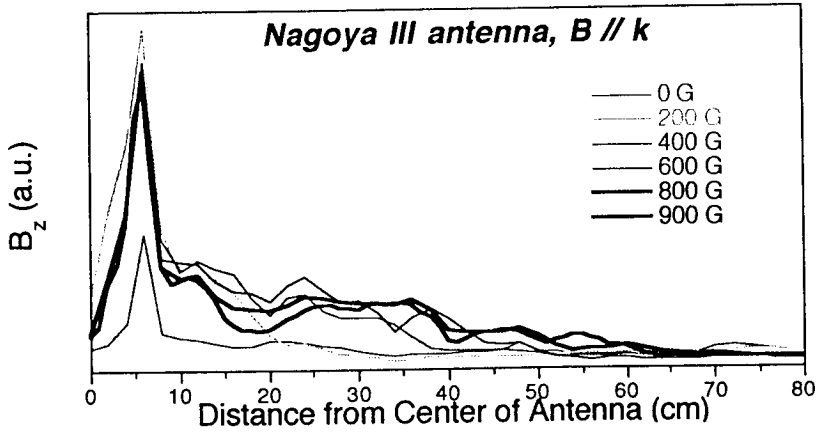

As was the case for the plasma emission and plasma density measurements, the standing wave pattern measured depends on the direction of the axial magnetic field. These patterns confirm that at these power levels helical antennas efficiently excite the m=+1 azimuthal helicon mode but fail to couple to the m=-1 mode.

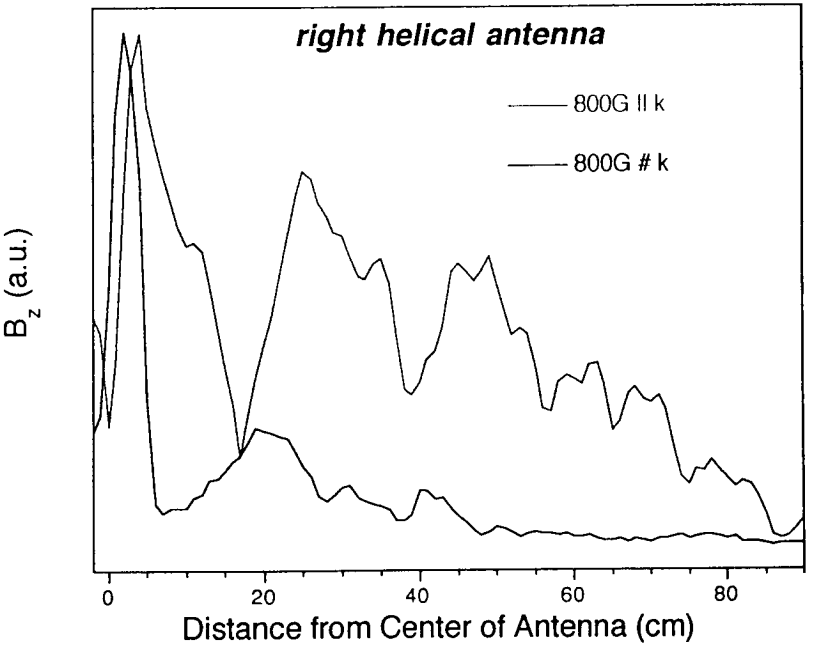

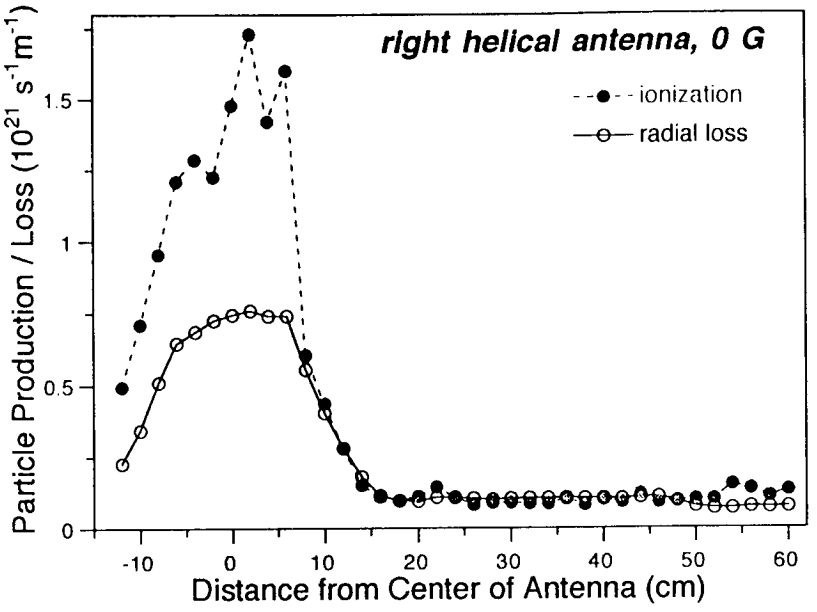

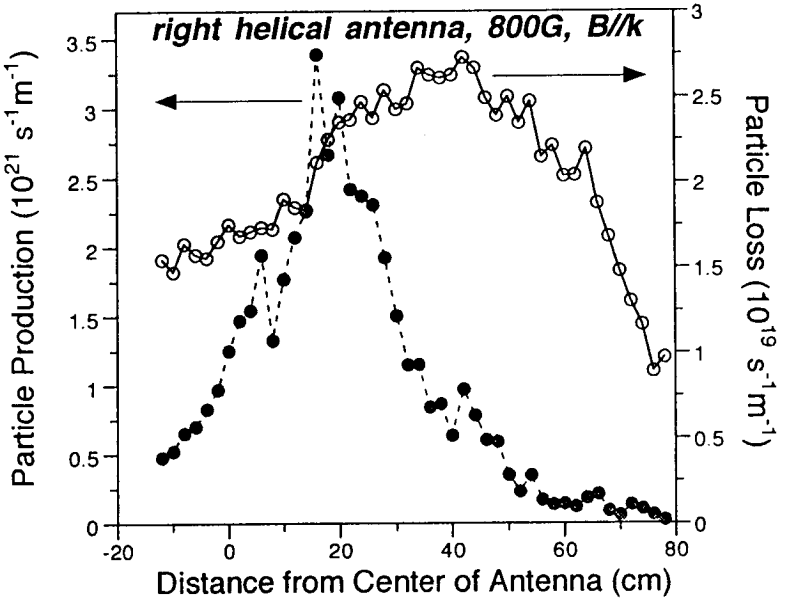

Helicon discharge operated with 15 mTorr of Ar gas, 2.0 kW of 27.12 MHz RF power, and various axial magnetic fields.

	B = 0 G	B = 800 G	B = 800 G*
Ionization rate (1/s)	3.14×10^{20}	9.4×10^{20}	2.36×10^{20}
Radial loss rate (1/s)	1.92×10^{20}	0.18×10^{20}	0.74×10^{20}
Input power (kW)	2.0	2.0	2.0
Power lost through volume ioniaztion (kW)	3.2	11	2.8
Power lost through radial losses (kW)	2.0	0.21	0.86

*Corrected for reduced neutral pressure during discharge operation.

The steady state equation of continuity for either species is:

$$Nn(r,z)\overline{\sigma_i v(z)} = -\nabla \bullet (D_a \nabla n)$$

N = neutral density
σ_i = ionization cross section
D_a = ambipolar diffusion coefficient

This equation can be integrated over the volume of the plasma:

$$N\int_0^L \overline{\sigma_i v(z)}\left[\int_0^a n(r,z)2\pi r dr\right]dz = 2\pi a\int_0^L D_a(a,z)\left[\frac{\partial n(r,z)}{\partial r}\right]_{r=a} dz$$

The left hand side of the equation corresponds to the volume-integrated particle production rate while the right hand side corresponds to the surface-integrated radial loss rate.
The measured plasma parameters can be used to calculate both production and radial loss rates.

The ambipolar diffusion coefficient is defined as:

$$D_a = \frac{\mu_e D_i + \mu_i D_e}{\mu_e + \mu_e}$$

for $\boldsymbol{B} = 0$ $\quad D_e(r,z) = D_{e\,\|} = {KT_e(z)}/{mv_e(r,z)}$

for $\boldsymbol{B} = 800$ G $\quad D_e(r,z) = D_{e\,\perp} = {D_{e\,\|}}/{(1 + \omega_c^2 / \nu_e^2)}$

The effective collision frequency is defined as:

$$\nu_e(r,z) = \nu_{ei}(r,z) + \nu_{en}(z)$$
$$\nu_{ei}(r,z) = 2x10^{-6} n(r,z) \ln \Lambda T_e(z)^{-3/2}$$
$$\nu_{en}(z) = N\overline{\sigma_m V(z)}$$

Both the ionization rate and the radial loss rate can be used to estimate the power lost. The average energy ε_i consumed in creating each electron-ion pair (including inelastic excitations) is a calculable function of electron temperature. The total energy ε_t effectively carried out by each electron-ion pair lost is equal to:

$$\varepsilon_t(z) = 2KT_e(z) + \frac{1}{2}KT_e(z) + \frac{1}{2}KT_e(z)\ln\left(\frac{M}{2\pi m}\right) + \varepsilon_i(z)$$

The neutral pressure during the helicon discharge operation is lowered by the high degree of ionization and by the fact that the fraction of neutral gas that is ionized is pumped out at the ion acoustic velocity.

The plasma densities for various configurations have been compared. The peak density for standard ICP conditions is about an order of magnitude smaller than for helicon discharges. For different antenna geometries and magnetic field directions, the helicon plasma density is basically the same under the antenna but differs downstream. The highest density is achieved with the right helical antenna with parallel field, conditions conductive to the excitation of the m=+1 mode. A short plasma column is obtained when the field direction is reversed, indicating the failure to excite the m=-1 mode efficiently. The Nagoya III antenna plasma column falls in between these two cases.

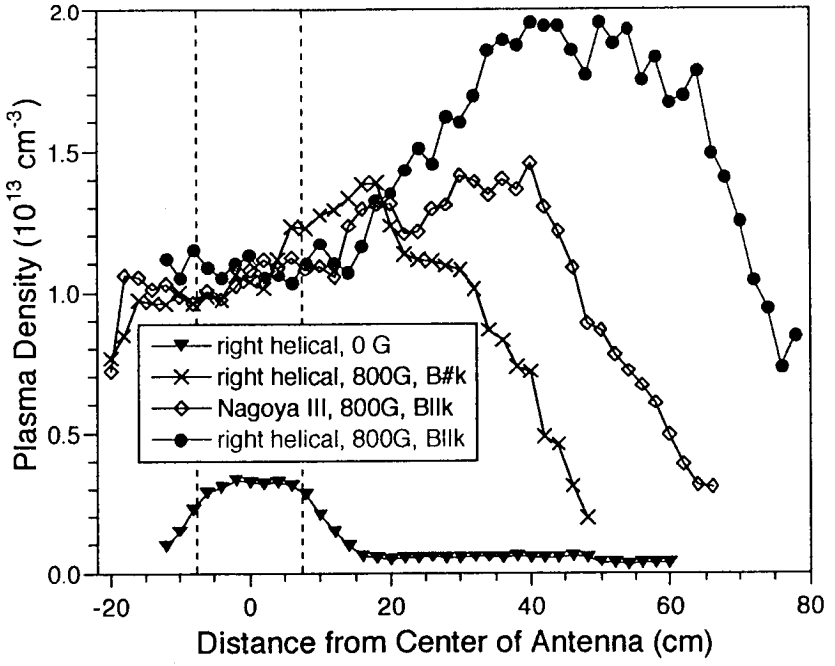

The axial density variation can be shown to follow from pressure balance. In steady state, the z component of the electron equation of motion is:

$$-enE_z - \frac{\partial (nKT_e)}{\partial z} - mn\nu_m u_z = 0$$

E_z = z component of the electric field

ν_m = momentum transfer collision frequency

u_z = z component of the electron fluid velocity

Measured electron temperature and density and plasma potential can be used to calculate the electric force and the pressure gradient force.

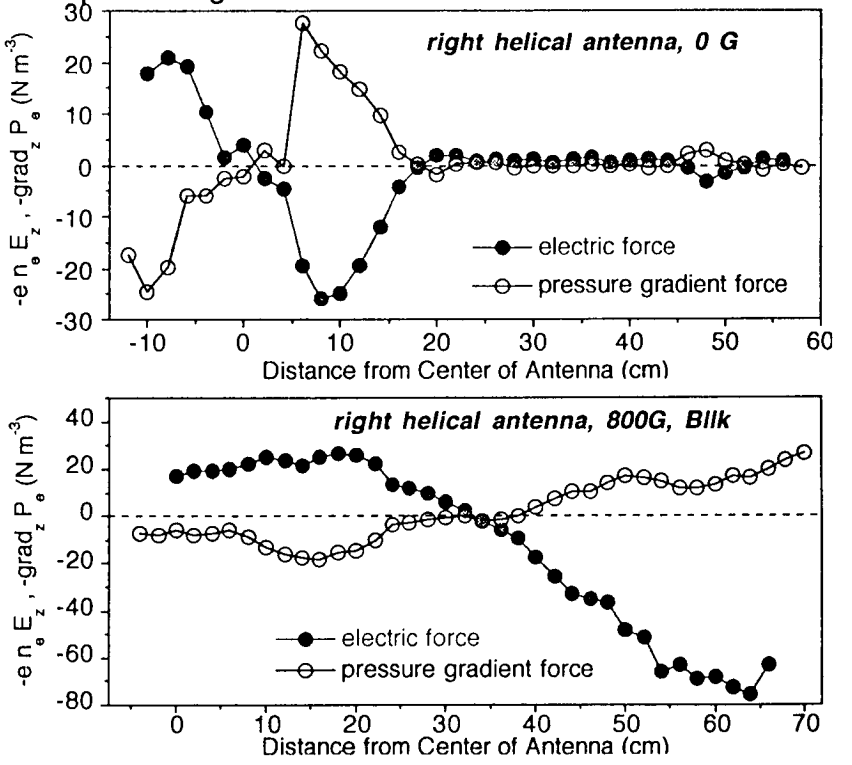

The 488 nm Ar^+ emission line corresponds to the transition $4p\ ^2D^0_{5/2}$ ----> $4s\ ^2P_{3/2}$. At the high-density, low-temperature plasma conditions we work with, the upper level is populated by electron emission impact excitation of the ground state of the Ar^+ ion. The emission intensity I_{em} is proportional to :

$$I_{em} \propto n^2(z)\ \overline{\sigma_x(z)\ v(z)}$$

n = plasma density
σ_x = cross section for impact excitation (Imre *et al.*)
v = electron speed
$\overline{\quad}$ = averaged over a Maxwellian electron velocity distribution with temperature $T_e(z)$.

Probe data has been used to predict the optical emission profiles.

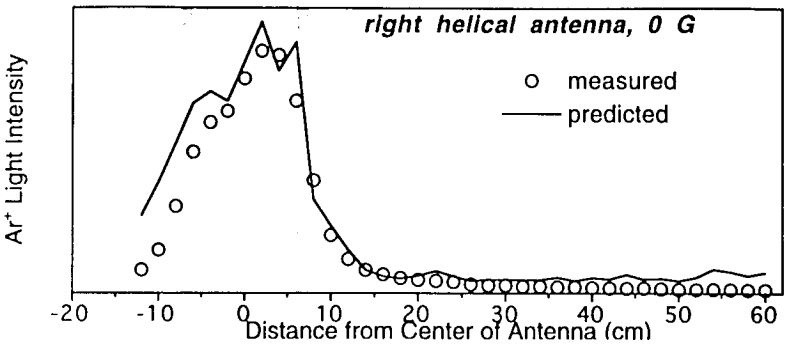

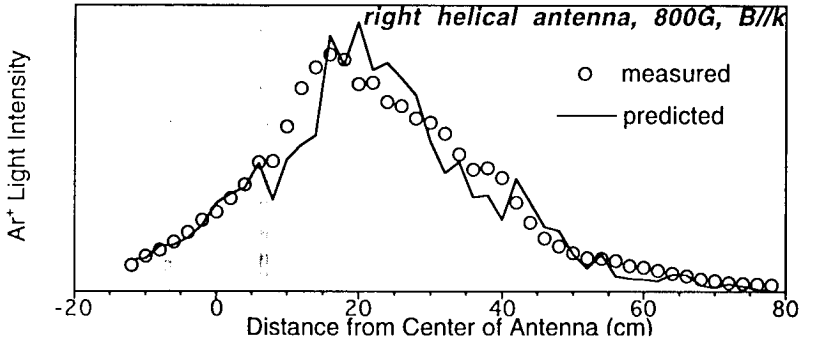

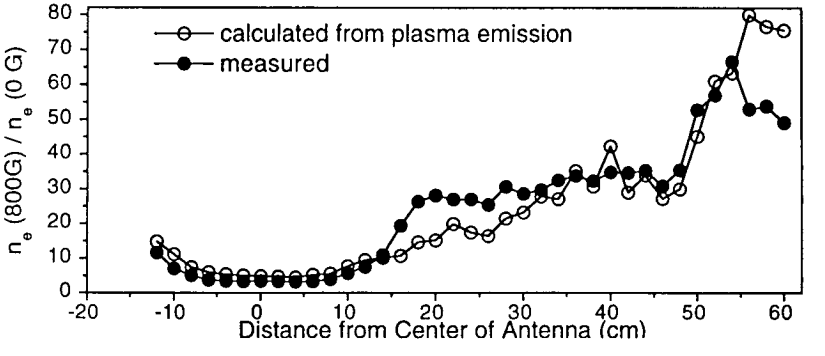

The dependence of plasma production on the magnetic field's direction was investigated. When two opposite field directions were used, the plasma emission peaks away from the antenna, in the direction of the magnetic field.

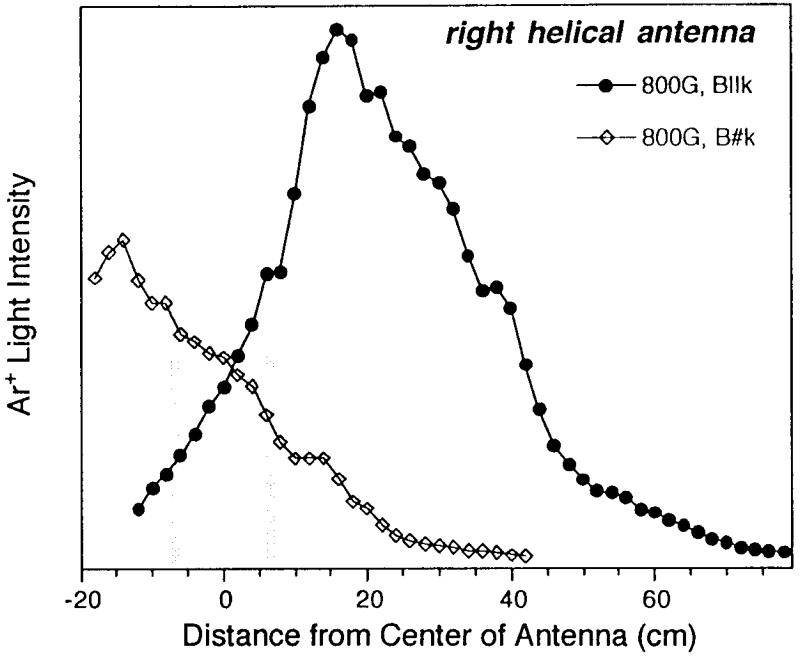

The axial profiles of the 488 nm Ar^+ line for a Nagoya III antenna with zero magnetic field and two directions of magnetic field are presented. In contrast to the rigth helical antenna, all the profiles ar fairly symmetric, with one central peak within the antenna region, and two peaks 16 cm from the center of the antenna. Plasma production seems to be insensitive to field direction.

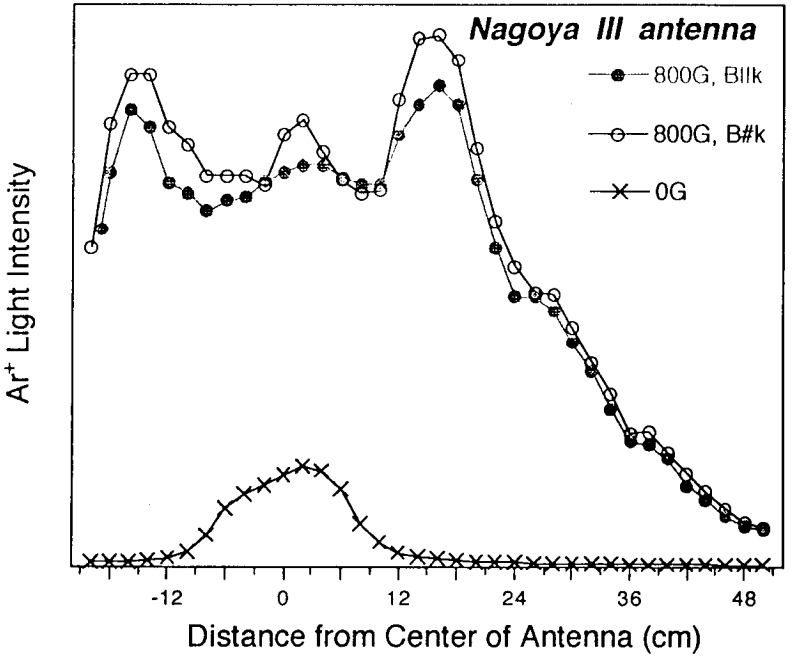

The electron temperature and plasma density as a function of distance from the center of the antenna for the standard ICP (no axial field) mode of the helicon discharge were measured. The density is symmetric about the center of the antenna, peaking there. This location has also the highest electron temperature. As the plasma diffuses out of the antenna region, it cools down.

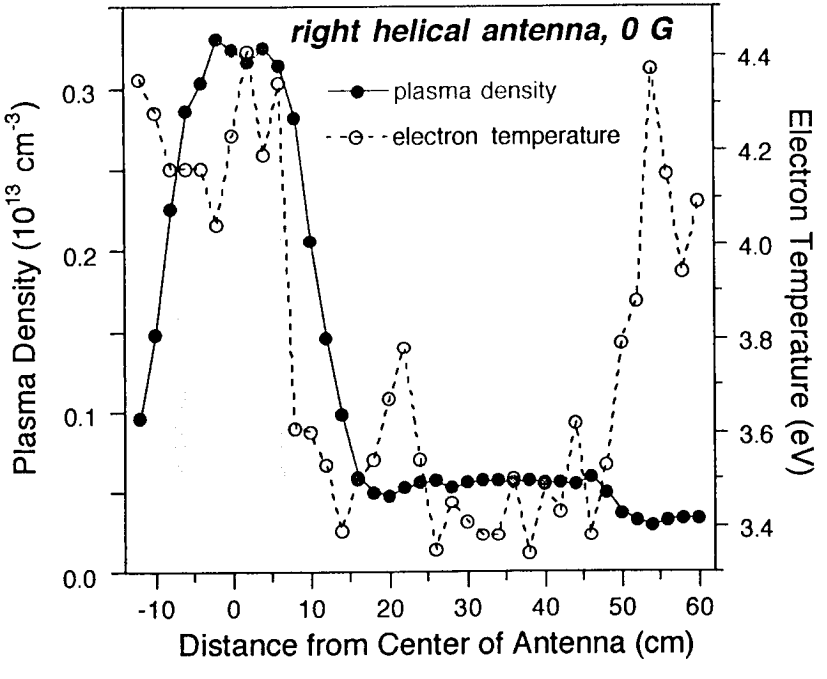

In the helicon mode with ***B // k*** the electron temperature peaks 16 cm from the center of the antenna and cools downstream; the electron density is uniform within the antenna region and increases by a factor of two several antenna lengths (50 cm) downstream.

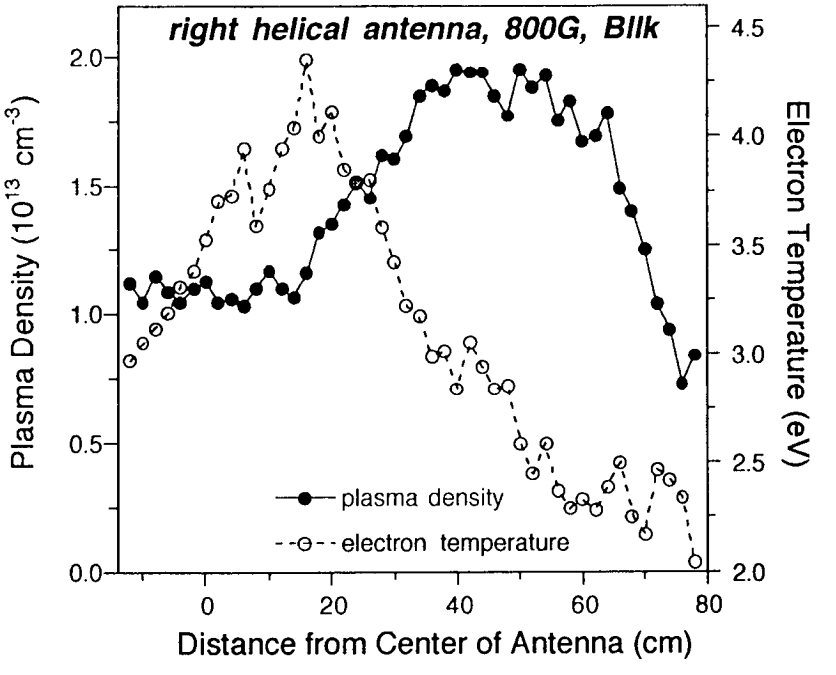

The axial dependence of the 488 nm Ar^+ plasma emission line at low magnetic fields is shown bellow for ***B // k*** . For zero field, there is a fairly symmetric emission profile within the antenna region. As the field is increased, however, two distinct peaks appear. The closest to the antenna is under the front ring while the second peak is located about 16 cm from the center of the antenna.

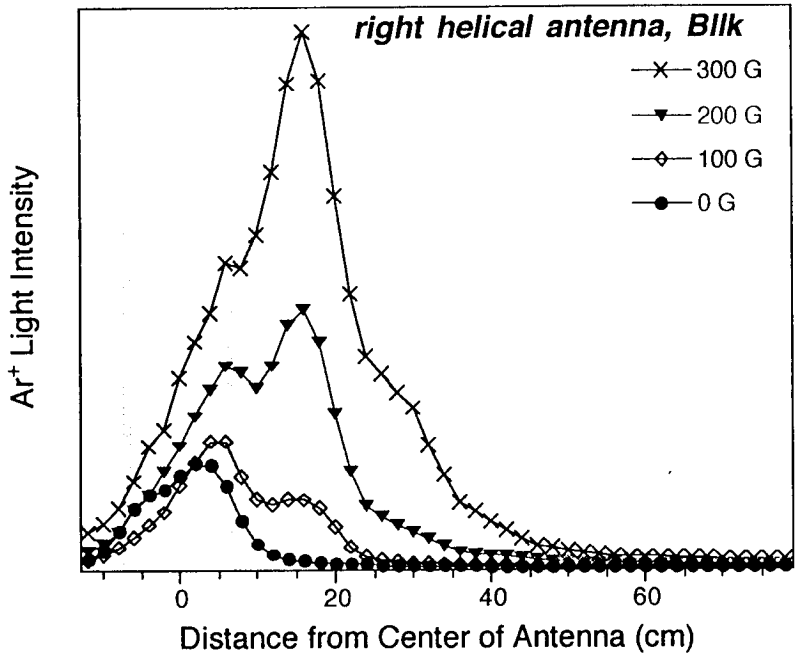

The profiles for magnetic fields from 0 to 900 G, at intervals of 100 G, reveal that the second (helicon) peak increases in magnitude but remains fixed in position. The emission profiles are very asymmetric with respect to the center of the antenna, suggesting preferential plasma production in the direction of the magnetic field for this antenna helicity.

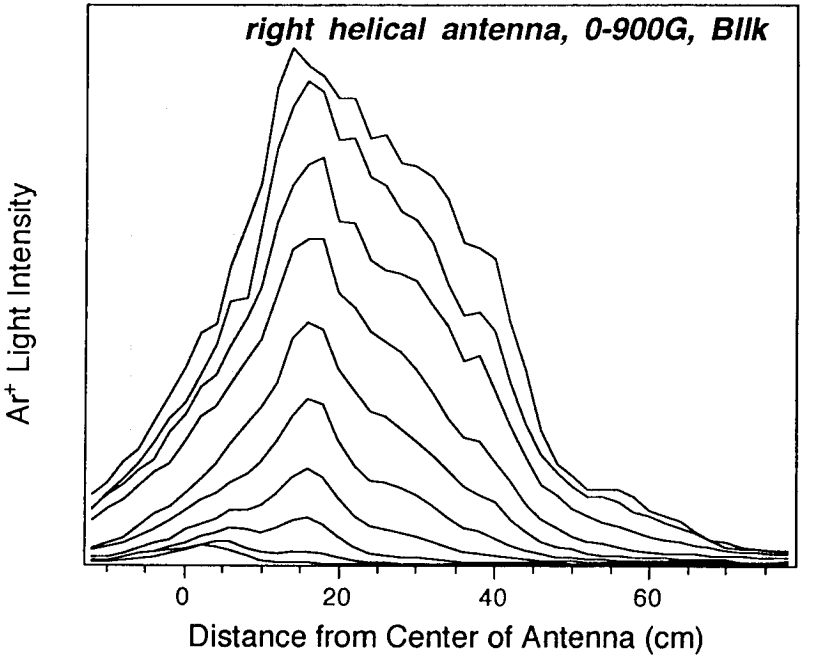

ABSTRACT

In the last two years, we have made great progress in understanding how helicon discharges work. Major results are:

1. We have solved the dispersion relation for nonuniform plasma densities. The measured density profiles are used henceforth.

2. The wave magnetic field has been measured radially for various antennas. The m = +1 azimuthal mode is preferentially excited and agrees well with theory.

3. The density, temperature, potential, and Ar II light have been measured axially for helical and straight antennas. The density peaks downstream. These data have been explained by a diffusion model of the discharge.

4. The wave magnetic field has been measured axially. The wavelength varies as expected with density. A standing wave pattern is seen which is explained by the beating of two radial modes. Antenna calculations support these observations.

5. The ANTENA code has been understood and simplified so that antenna coupling calculations can be made on a PC.

6. No Landau-accelerated fast electrons have been observed; our ionization can be explained by collisional damping alone.

7. Diagnostics have been developed and theoretically analyzed for the above measurements. A new theory shows that fast electrons which occur in pulses in phase with the RF cannot be seen with our RF-compensated Langmuir probes.

8. The helicon discharge appears to be an ideal remote source, with high density and low T_e downstream from the antenna.

Helicon Discharge:
15 mTorr Ar
2.0 kW